Landslides (2017) 14:1147–1160
DOI 10.1007/s10346-016-0792-5
Received: 1 August 2016
Accepted: 21 December 2016
Published online: 6 January 2017

Guo Wu · Dickson Cunningham · Ren-mao Yuan · Qing Zhou · Xinfu Zeng · Xiao-ping Yang

Mass-wasting effects induced by the 2015 Gorkha (Nepal) M_w 7.8 earthquake within a large paleo-landslide site adjacent to the Tatopani Border Station, Nepal: implications for future development along the critical Bhote Koshi River valley transport corridor between Nepal and China

Abstract The 2015 M_w 7.8 Gorkha earthquake and its aftershocks caused nearly 9000 deaths and more than 23,000 injuries and triggered thousands of landslides and other mass-wasting effects in the steep, rugged topography of Nepal. In this paper, new slope failures and tension cracks induced by the 2015 Nepal earthquake are documented in steep terrain west of the Tatopani Border Station, which lies along the deeply incised Bhote Koshi River valley, a critical trans-Himalayan transport route between south Asia and Tibet/China. The affected area west of the Tatopani station is the site of a large reactivated paleo-landslide that has experienced repeated failures. The Tatopani station is downslope from the amphitheater-like landslide scar and is constructed on distal landslide debris in a position vulnerable to future landslide and fluvial erosion hazards. We carried out detailed field investigations to document different types of geohazards around the station and present an evolutionary model for past and present landslide development. In addition, a simple numerical model was constructed to evaluate the stability of the large paleo-landslide body under different earthquake conditions. Simulated results suggest that the paleo-landslide body is stable without seismic loading. However, the large paleo-landslide will be remobilized again by large slope failures if the PGA of future earthquake exceeds 0.35 *g*. We suggest that the results presented in this paper should be taken into consideration during earthquake-resistant design of the border station and other infrastructural development along the Bhote Koshi Valley.

Keywords 2015 M_w 7.8 Gorkha earthquake · Landslide hazards · Mass wasting · Stability analysis · Himalaya, Tatopani Border Station

Introduction

The M_w 7.8 Gorkha (Nepal) earthquake occurred on April 25, 2015, in the central Himalaya and was followed by a series of M >6 aftershocks, including the M_w 7.3 event on May 12, 2015 (Fig. 1). The Gorkha earthquake sequence resulted in nearly 9000 deaths and more than 23,000 injuries. The earthquakes also triggered thousands of landslides and other mass-wasting effects in the steep, rugged topography of Nepal (Collins and Jibson 2015; Hashash et al. 2015; Kargel et al. 2016).

The Tatopani Border Station of Nepal is located on the most significant road connection between Nepal and China (Araniko Highway). The Zhangmu Border Station of the Tibetan province of China is 6 km further north up the Bhote Koshi River Valley (Fig. 1). The Tatopani Border Station was constructed within the narrow confines of the Bhote Koshi River valley on distal deposits of a large paleo-landslide (Fig. 1). The landslide area above Tatopani was partly reactivated during the 2015 M_w 7.8 Gorkha (Nepal) earthquake. Therefore, in order to assess current and future geohazards around the Tatopani border station area, a detailed field investigation was carried out during June 2015. This paper summarizes the results of that investigation.

In this paper, geomorphological features of the large preexisting landslide are documented and the potential effects of the reactivated landslide on the station are discussed. An evolutionary model of the landslide's development is provided based on documentation of the geomorphological and geological site conditions. In addition, the stability of the landslide under different potential earthquake conditions is analyzed using a two-dimensional numerical model. The results are helpful for geological hazard mitigation in the area around the Tatopani station.

Regional geological and geomorphological setting

The Himalaya comprises a stack of thrust sheets (Le Fort 1975) that is traditionally divided into the Tibetan Himalaya, Greater Himalaya, Lesser Himalaya, and Sub-Himalaya zones. The major fault systems that separate these zones are the South Tibetan Detachment System (STDS) between the Tibetan and Greater Himalayas, the Main Central Thrust (MCT) between the Greater and Lesser Himalayas, the Main Boundary Thrust (MBT) between the Lesser Himalaya and Sub-Himalaya, and the Main Frontal Thrust (MFT; Fig. 1; Gansser 1964). The Main Himalayan Thrust (MHT), which corresponds to the subsurface expression of the MFT absorbs about 15–20 mm/year of convergence within Nepal, which is nearly half of the present convergence between the India and Eurasian plates (Bilham et al. 1997; Bettinelli et al. 2006; Mugnier and Huyghe 2006).

Earthquakes along the Himalayan fault systems release strain energy that causes severe surface damage and mass-wasting effects. In the Nepalese Himalaya, prior to 2015, historical earthquakes with large magnitudes were mainly recorded in the east and west, whereas a seismic gap was documented in the central segment (Shanker and Sharma 1998; Ader et al. 2012).

Nearly 83% of Nepal's total area is mountainous and/or hilly. The continued collision of the Indian and Eurasian plates causes seismogenic thrust faulting that generates mountain building characterized by rugged topography, high relief, steep slopes, deeply incised river valleys and variable climatic conditions including intense monsoonal precipitation (Hasegawa et al. 2009). Himalayan topography is prone to landslides and erosion and

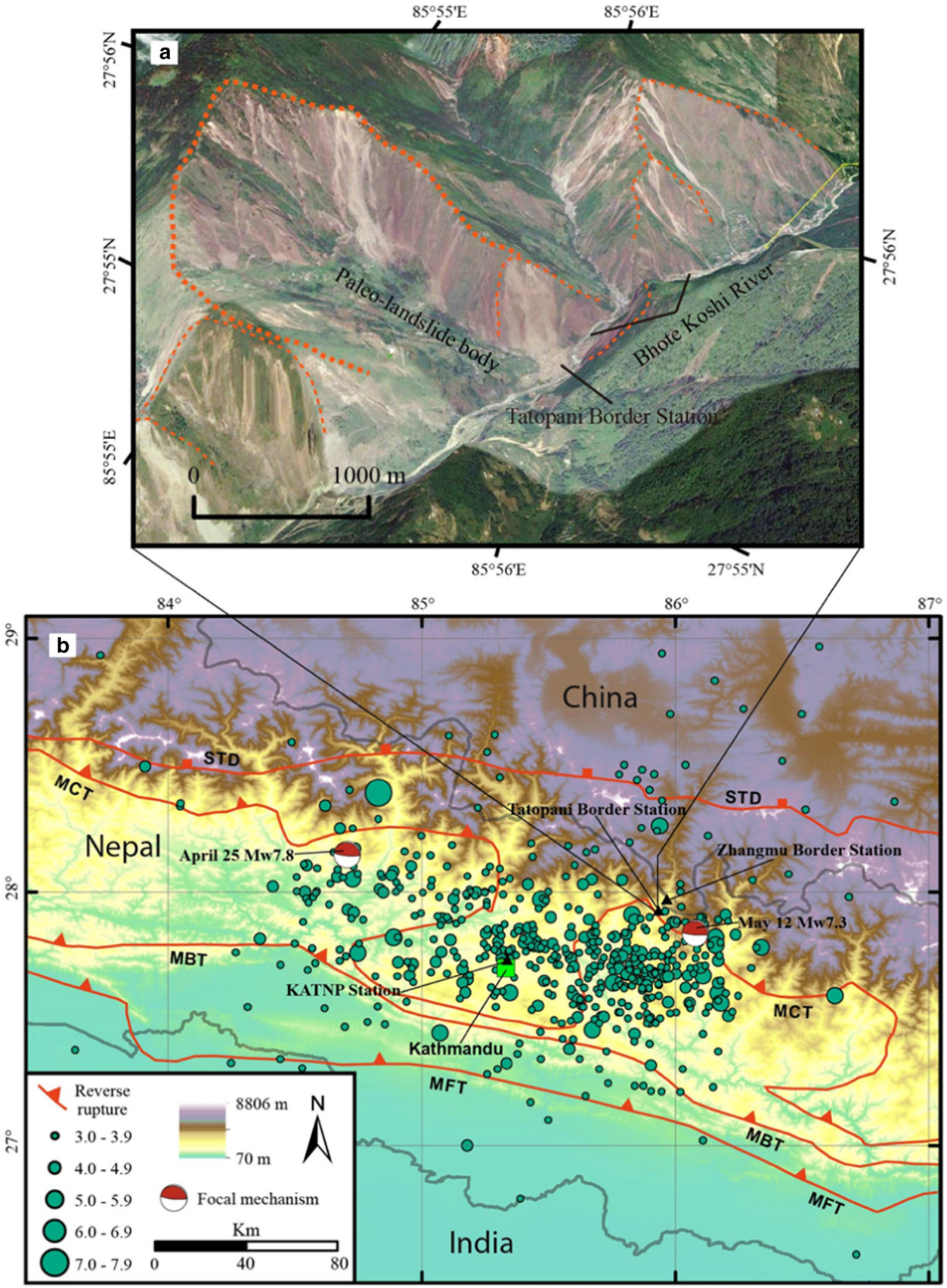

Fig. 1 Distribution of the Gorkha earthquake sequence and location of the Tatopani Border Station in Nepal (http://www.isc.ac.uk, International Seismological Centre, ISC). *MFT* main frontal thrust, *MBT* main boundary thrust, *MCT* main central thrust, *STD* south tibet detachment. *Top image* shows Google Earth image of landslide area directly west and upslope of Tatopani Border Station

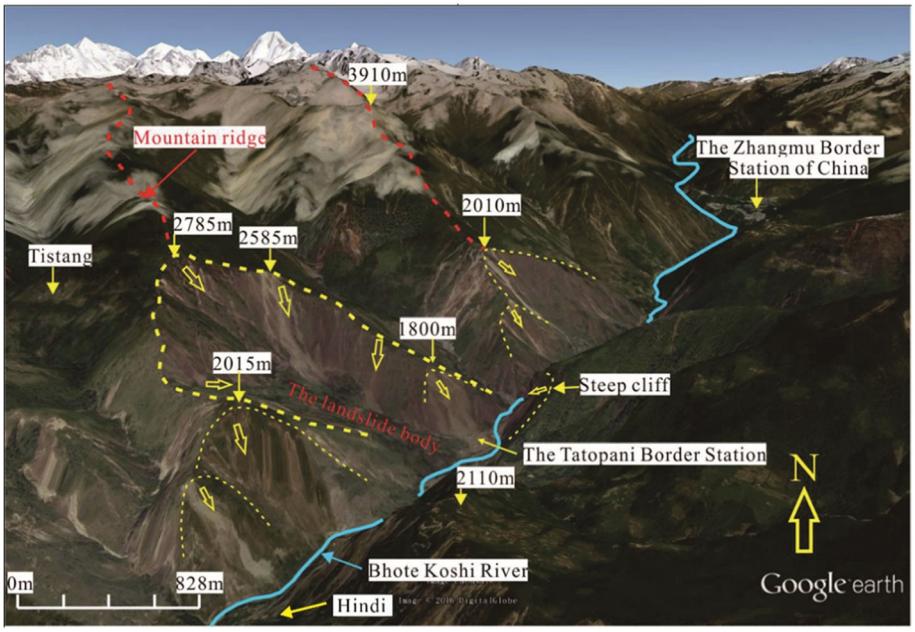

Fig. 2 Oblique N-looking perspective of the Bhote Koshi River valley and region surrounding the Tatopani Border Station of Nepal. *Yellow arrows* indicate directions of landslide movements

about 12,000 small- and large-scale landslides occur in Nepal every year (Bhattarai et al. 2002).

The Tatopani Border Station of Nepal is located on the west bank of the Bhote Koshi River (Figs. 1 and 2) which originates from the Tibetan Plateau and has incised a deep valley through the Himalaya. The N-S valley is bordered by steep slopes and cliffs on both its east and west sides for most of its length. The valley is a significant trade route and links the development of Nepal with Tibet.

The Tatopani station is located at the toe of a paleo-landslide deposit (Figs. 1b and 2) in a narrow section of the valley. The elevation of the site is 1370 m and elevations of surrounding ridgelines range from 1800 to 3000 m with up to 1600 m of relief in the immediate vicinity. The west side of the station is bordered by a steep 65–70° slope that rises 430–650 m above the station, whereas a 640-m-high cliff is on the east side of the station (Fig. 2).

The rock mass in the investigation area is mainly composed of phyllite. Asymmetric hillslope topography reflects the attitude of the phyllite foliation which is usually 30–40° for the dip slope and 45–60° for the scarp slope. At the site area, diamicton (unconsolidated landslide debris) is interbedded with fluvial deposits.

Phyllite is mainly composed of mica, quartz, and chlorite and has relatively high shear strength in its intact state. However, the phyllite in the study area is highly weathered and friable, especially on the ridge tops and cliff faces. Three sets of discontinues are present (Fig. 3): phyllite foliation planes which dip 39°/001° (Fig. 3a) and two sets of joints dipping 70°/115° and 65°/190° (Fig. 3b). The density of planar discontinuities in the phyllite and high concentration of mechanically weak mica, coupled with episodic seismic ground shaking and steep terrain, has predisposed the bedrock to landslides and other mass wasting effects.

Geohazards around the Tatopani Border Station

The steep slopes, weathered bedrock, and intense monsoonal rainfall of the Nepalese Himalaya create ideal conditions for geohazards (Gabet et al. 2004). Landslides are a primary agent of hillslope degradation and constitute one end of the spectrum of slope modification processes in the Himalayan region (Shroder and Bishop 1998; Hasegawa et al. 2009). Along the Bhote Koshi River valley, different geohazards exist in the area surrounding the Tatopani Border Station (Figs. 2 and 4a; Bhandary et al. 2013), including landslides, rockfalls, and other

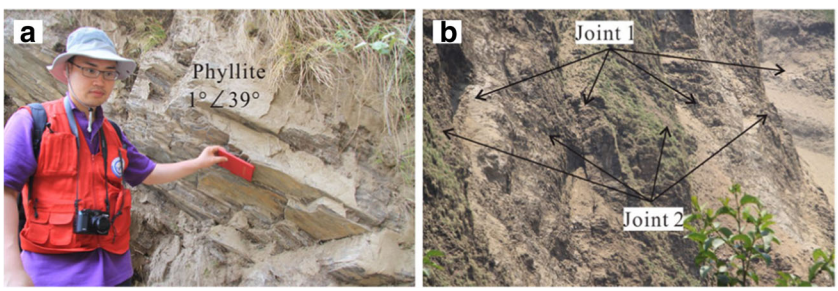

Fig. 3 Photos of the phyllitic bedrock and its major structural discontinuities. **a** Moderately dipping phyllite. **b** Two sets of joints in phyllite (View looking to NE; *1* and *2* shown in Fig. 4b are the locations of **a** and **b**)

collapse phenomena; flooding; and river erosion. The station was constructed on older landslide materials downslope from the steep amphitheater-like landslide source area (Fig. 4b). The 2015 M_w 7.8 Gorkha earthquake and its aftershocks caused additional mass wasting and detrimentally affected the stability and safety of the border station.

Because of extreme topographic differences from south to north, the climate in Nepal is highly variable with significant differences in mean annual precipitation. The annual amount of precipitation, 80% of which takes place in a period of about 4 months from mid-May to mid-September, varies from less than 250 mm in the north of the Himalayan range to around 6000 mm

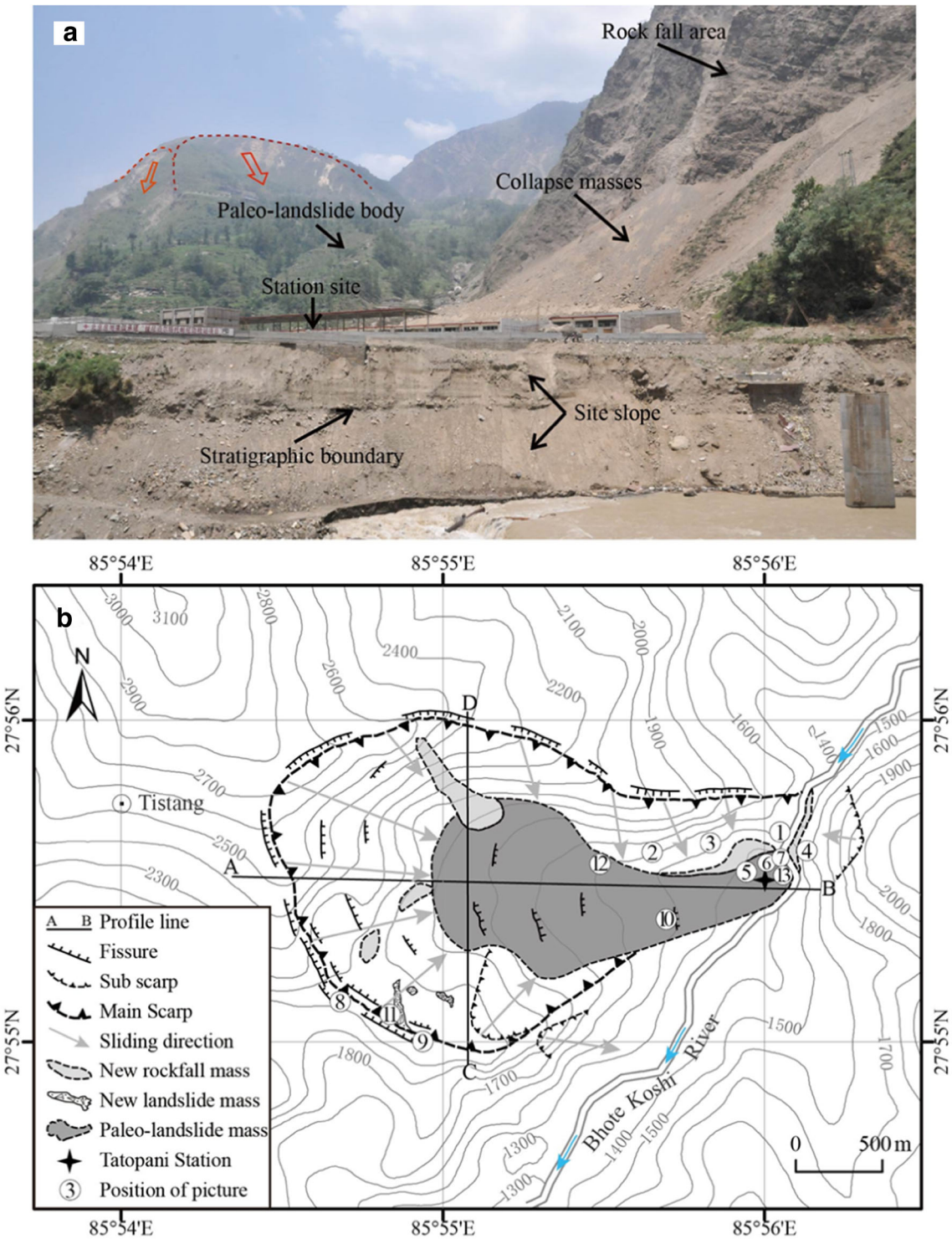

Fig. 4 Geo-hazards around the area of the Tatopani station site: **a** View looking SW of recent landslide evidence directly above and adjacent to border station site; **b** Sketch map of the large paleo-landslide west of Tatopani Border Station. See Fig. 5 for geological profile line A-B and Fig. 6 for line C-D

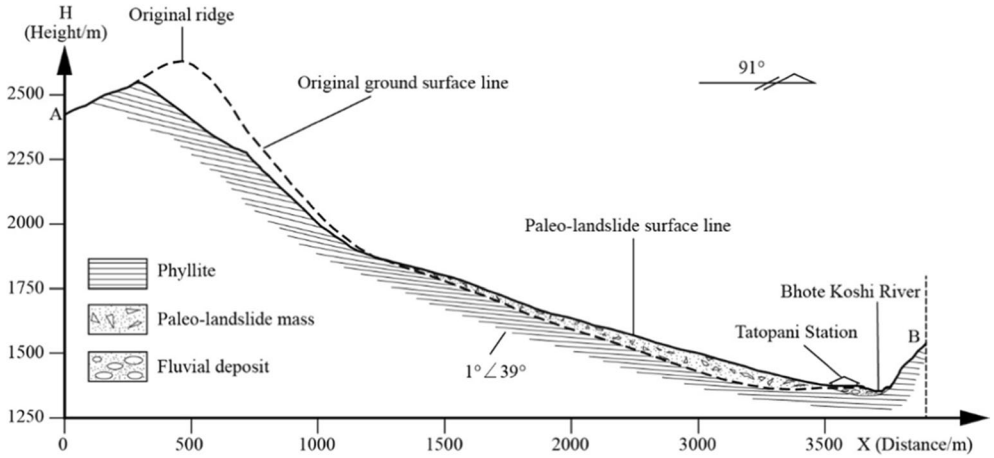

Fig. 5 View N of geologic profile (A-B) of the large paleo-landslide west of Tatopani (profile line shown in Fig. 4b). No vertical exaggeration

at Lumle in central Nepal. According to the 24-h maximum rainfall map of Nepal provided by the Nepalese government's Department of Hydrology and Meteorology, the annual rainfall in the area of the Tatopani Station is typically 250–300 mm (Bhandary et al. 2013). Although the mean annual precipitation in northern Nepal is not very high, it is highly concentrated during the rainy season. During the summer monsoon, Bhote Koshi River volumes are highest and erosional power is greatest (Bhandary et al. 2013).

Due to the large landslide deposits that emanated from the major paleo-landslide zone west of the Tatopani Station which flowed downslope into the Bhote Koshi River valley, the river was forced to shift its channel eastward. The west side of the river thus became its convex-outward bank (Figs. 2 and 4) which are susceptible to focused erosion at the bank's northern end (Fig. 4a, b). This presents an ongoing threat to the long-term stability of the unconsolidated sediments that the station is built upon.

Paleo-landslides at Tatopani Border Station

In the investigation area, three landslide groups occur near the station mainly on the west bank of the Bhote Koshi River (Fig. 2). Field and remote sensing investigations indicate that these landslide bodies are covered by grass, shrubs, and trees, indicating that they are paleo-landslides. All of the main landslide breakaway scarps cut the mountain ridge lines. The middle landslide (Fig. 2) is the largest and the Tatopani station is located on its most distal deposits. The flatter ground of the sedimentary deposits is topographically favorable for the station site. However, the stability of the landslide sediments directly affects the suitability of the station and the safety of its inhabitants (Figs. 2 and 4).

This large landslide is about 2.6 km wide and 1.8 km long and moved toward the east, clogging the river and diverting its channel (Figs. 2 and 4b). A large portion of the mountainous mass on the west bank of the river was destroyed by this landslide (Figs. 2 and 4). The main scarp defines an irregular circular shape, and subscarps were also developed on the south part of the landslide area. The north part of the main scarp forms a high cliff, which is susceptible to further collapse.

Geological and topographic characteristics of the large paleo-landslide west of Tatopani Station

The geologic profile (A-B; Fig. 5), which is parallel to the downslope sliding direction of the landslide, reveals that the main breakaway scarp at upper elevations is inclined at approximately 45° and much steeper than the surface slope of the lower accumulation area. The top elevation of the main

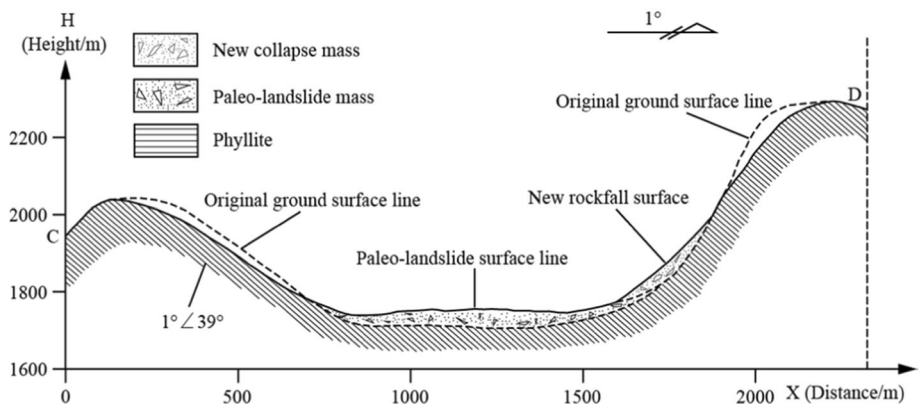

Fig. 6 Geologic profile (C-D) of the large paleo-landslide (profile line is shown in Fig. 4b)

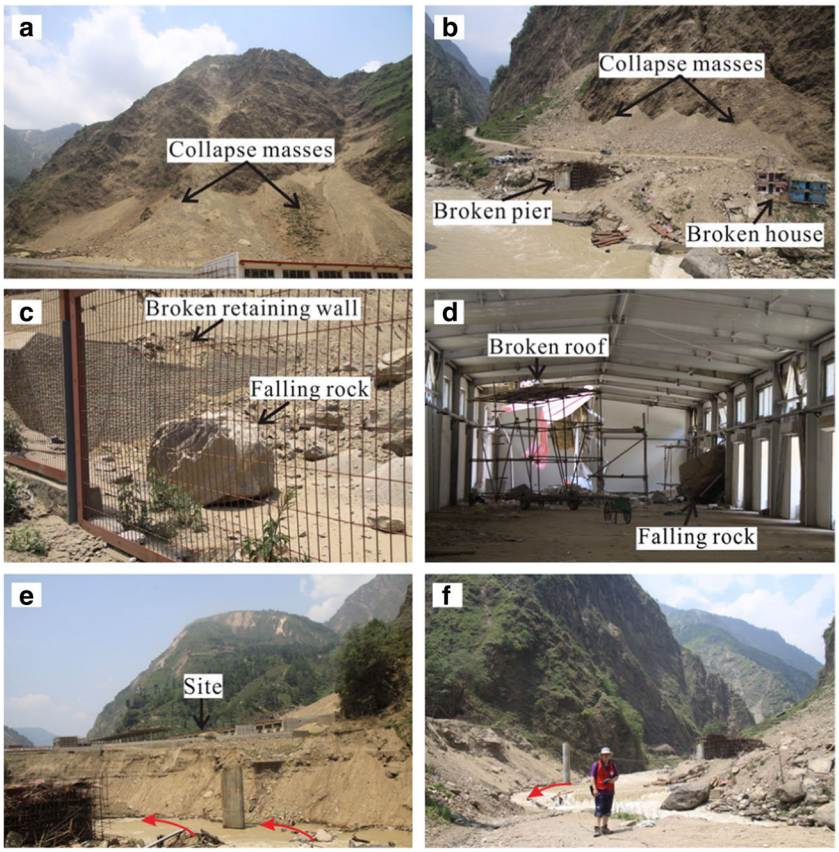

Fig. 7 Collapse features and river erosion along the Bhote Koshi River: **a**, **b** fresh talus from slope collapse along the west and east cliffs (view looking to NW in **a** and NE in **b**; locations of **a** and **b** shown in Fig. 4b are points *3* and *4*, respectively); **c**, **d** damaged retaining wall and warehouse after 2015 Nepal earthquake (locations of **c** and **d** = points *5* and *6* in Fig. 4b, respectively); **e**, **f** river bank erosion (*red arrows*) along the Bhote Koshi River (view looking to SW; their locations are close to point *7* in Fig. 4b)

breakaway scarp is 2780 m, which is 1400 m above the station. It is worth noting that the sliding surface cut through the mountain top and removed its former summit. This likely suggests that the main landslide was triggered by a large magnitude earthquake instead of monsoonal saturation of near-surface materials.

According to profile C-D (Fig. 6), boundary scarps along the N and S sides are very different (Fig. 6). The southern bounding scarp is relatively gently inclined at about 30°. This slope is weathered and eroded and may have been steeper, reflecting the dip of the underlying phyllite (Fig. 3a). On the other hand, the northern bounding scarp is more steeply inclined at about 60°, forming a

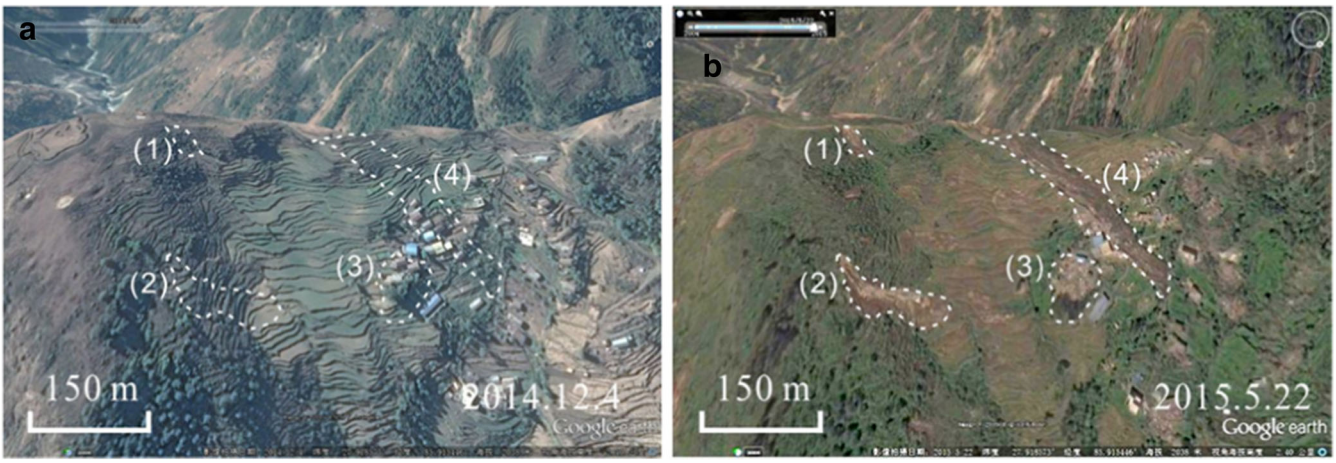

Fig. 8 Contrast images of the landslide area before (**a**) and after (**b**) the 2015 Gorkha earthquake (view looking to the southeast)

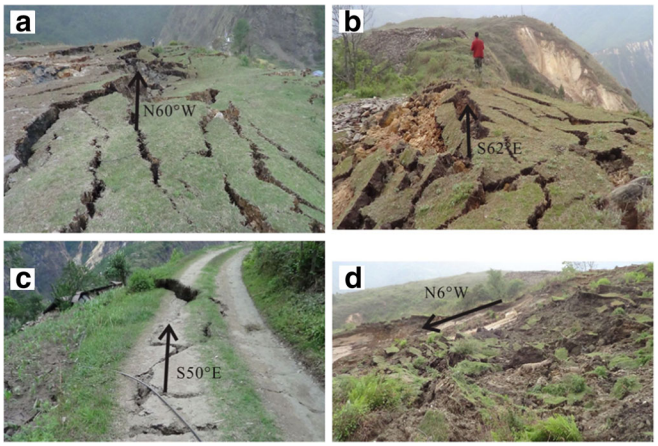

Fig. 9 Tension cracks and secondary landslide effects triggered by the 2015 M_w 7.8 Nepal earthquake in the large paleo-landslide area west of Tatopani Border Station. **a**, **b** Tension cracks along the southwest scarp. **c** Tension cracks in the middle-lower part of older landslide deposits. **d** Rear area of the largest secondary landslide (*8*, *9*, *10*, and *11* in Fig. 4b are the positions of photos *a*, *b*, *c* and *d*, respectively)

cliff that is prone to collapse. This steeper scarp appears to be mainly controlled by joints in the phyllite (Fig. 3b).

New mass-wasting effects within the large paleo-landslide area induced by the 2015 Nepal earthquake sequence

During the 2015 M_w 7.8 Nepal earthquake, the large paleo-landslide area west of the Tatopani Station experienced renewed mass wasting along older scarps and within older landslide deposits, including some small- to medium-size landslides and development of numerous tension cracks (Figs. 7, 8, and 9). Field observations along profile C-D (Fig. 6) revealed that new rock falls and cliff collapses occurred mainly along the northern bounding scarps, whereas secondary landslides are more common along the southern bounding scarp (Fig. 4).

Figure 8 shows the large paleo-landslide area before and after the 2015 earthquake. The largest new landslide is 450 m long × 30 m wide and is visible as a narrow strip. It moved from the ridgetop and destroyed all the terraced fields and residential buildings in its path (Fig. 8). The secondary landslides are shallow and displaced weathered bedrock and unconsolidated materials deposited from previous landslides (Fig. 9d).

Most of the earthquake-induced tension cracks occurred along the main scarps in the southwestern paleo-landslide area (Figs. 4 and 9a, b). They are typically tens of meters long and parallel to the trend of the mountain ridge. In addition, some new tension cracks formed in the middle-lower part of the main landslide body (Fig. 9c), but they are not as large and densely developed as the fissures along the main scarps. These new tension cracks may continue to develop with future earthquakes and potentially widen by future rainfall and associated erosion.

Two overhanging rock cliffs occur on both sides of the Bhote Koshi River near the station (Figs. 2 and 4). The west cliff, which is a steep scarp formed by the large paleo-landslide, is located northwest of the station. There is about 500 m of altitude difference between the top of the cliff and the station site. The Araniko Highway is at the foot of the east cliff, east of the river, and is connected to the Tatopani station by an iron chain bridge. Serious collapse hazards continue to exist from both cliffs; rock falls continued to occur during our field investigation in June 2015, 1–2 months after the main Gorkha shocks (Figs. 7a, b).

Because of the high and steep western cliff, a stable retaining wall was built before construction of the station. However, it was seriously damaged and partly buried by collapsed material during the 2015 Nepal earthquake (Figs. 7a, c). The workers' dormitory at the western corner of the station was also completely destroyed by huge fallen rocks. It was fortunate that the workers rushed out of the dormitory a few seconds before the rocks arrived. One 2.5-m diameter boulder that fell from the cliff hit the parking area and then rebounded to destroy the warehouse (Fig. 7d).

Slope collapses also occurred along the eastern cliff of the river valley during the earthquake (Fig. 7b), where the elevation of the cliff top is about 2040 m, more than 600 m higher than the Araniko Highway. Figure 7b shows a recently built

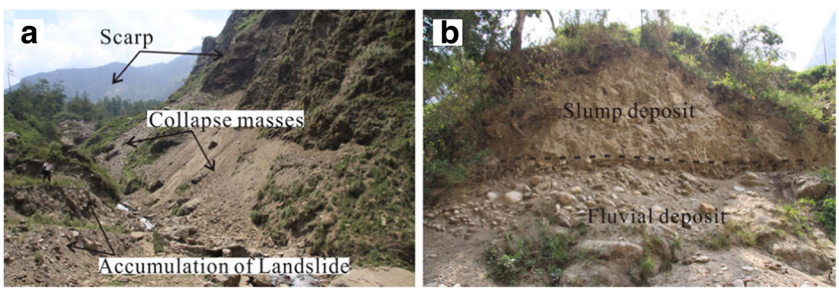

Fig. 10 **a** Older landslide deposits overlain by 2015 collapse deposits; **b** stratigraphic boundary between landslide accumulations and fluvial deposits (view looking to W; points *12* and *13* in Fig. 4b are the locations of **a** and **b**, respectively)

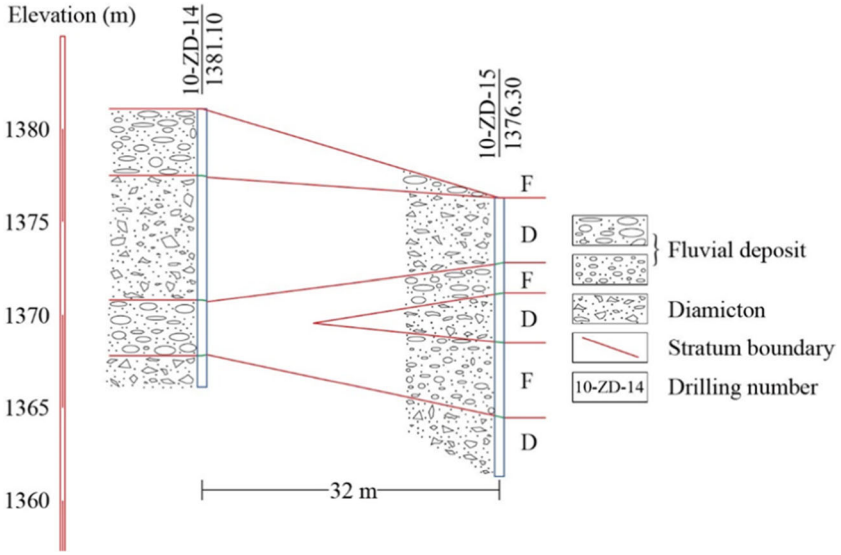

Fig. 11 Geologic profile at the site of the station (point *13* in Fig. 4b is close to the position of the borehole)

pier and several residential buildings that were destroyed or buried by the collapsed material, which also blocked the Araniko Highway.

In summary, new slope failures, rock falls, and tension cracks associated with the 2015 M_w 7.8 earthquake within the paleo-landslide area corroborate our concern that the Tatopani station lies in a position vulnerable to future landslide hazards.

Evolutionary model for the large landslide west of Tatopani

Landslide deposits at the Tatopani station

The large paleo-landslide mass is surrounded by large scarps and extends downslope to the Bhote Koshi River (Figs. 2 and 4). Field observations indicate that the debris in the accumulation area is composed of phyllite and some slate. The material is unconsolidated, angular, and unsorted and consists of very fine-grained sediment to very coarse boulder clasts (Fig. 8a). On the west bank of the Bhote Koshi River, fluvial deposits were overlapped by the landslide debris and the contact is clearly exposed (Figs. 4a and 10b).

The sedimentary stratigraphy of the Tatopani Station site was documented by studying field exposures (Fig. 10b) and by analyzing core and cuttings from several boreholes. The sedimentary succession at the toe of the landslide area consists of alternating diamicton and fluvial deposits separated by distinctive contacts (Fig. 11).

The upper layer consists of poorly sorted diamicton dominated by phyllite breccia and soil, representing the most recent deposits of the large paleo-landslide. It overlies a pebbly and coarse sandy layer interpreted as a fluvial deposit. At deeper levels, alternating diamicton and river deposits are found. This indicates that repeated landslide events have shifted clastic debris down to the lowest valley levels in the past (Fig. 11). The new slope failures that occurred during the 2015 M_w 7.8 Nepal earthquake indicate that the downslope displacement of landslide debris continues to be an ongoing, episodic process at the Tatopani site.

Evolutionary model for the large landslide west of Tatopani

Landslides are the most widespread geohazard type and the primary agent of hillslope erosion in the Nepalese Himalaya (Shroder and Bishop 1998). Alternations of landslide and fluvial sediment successions at the station site indicate that the large paleo-landslide west of the station has experienced a long-term and complex evolutionary process. A simple model is proposed to describe the landslide's evolutionary development based on the

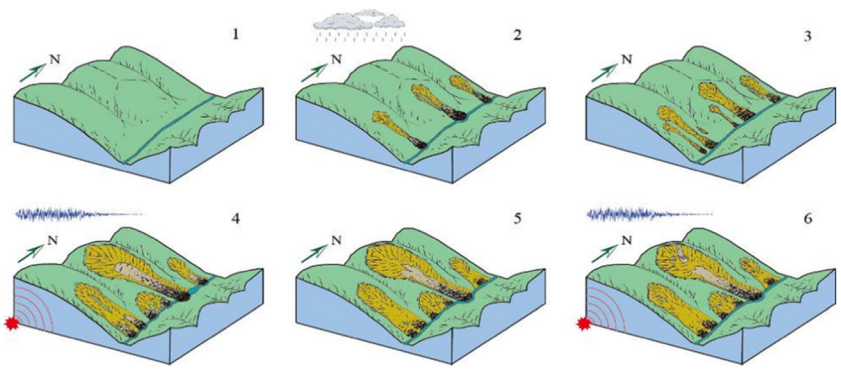

Fig. 12 Evolutionary model of the landslide area

Table 1 Material properties for simulation

Physical parameter	Paleo-landslide mass	Bedrock
Unit weight γ_t (kN/m^3)	20	24.5
Friction angle Φ (deg)	30	35
Cohesion C (kPa)	12	300
Possion's ratio μ	0.30	0.22
Damping ratio D_s	0.1	0.1
Young's modulus E (kPa)	60,000	2,400,000
Shear modulus G_{max} (kPa)	23,000	980,000

geomorphological and geological conditions documented at the site (Fig. 12).

Continued tectonism in the central Nepalese Himalaya has created mountainous topography with high relief and steep slopes, especially where antecedent rivers such as the Bhote Koshi have continued to incise during topographic and rock uplift (Fig. 12 (1)). During stage 2 in the Tatopani area, small to medium-size precipitation-induced landslides may have occurred on the east slope of the mountain west of the station and the materials likely temporarily blocked the Bhote Koshi River (Fig. 12 (2)). During stage 3, the river cut a new channel through the landslide debris (Fig. 12 (3)). During stage 4, ground shaking due to a large-magnitude earthquake caused significant failure of the mountain slope west of the station and the main breakaway scarp cut through the mountain ridge. The lobe of landslide debris blocked the river so that preexisting river deposits were covered by a layer of landslide debris (Fig. 12 (4)). Subsequently, a new succession of fluvial sediments was deposited behind the temporary debris dam, before the river cut through the landslide materials again. A new succession of fluvial deposits was then deposited above the landslide materials (Fig. 12 (5)). During the 2015 Gorkha (Nepal) M_w 7.8 earthquake, the large landslide was reactivated by the severe ground shaking. Secondary landslides occurred in the main landslide area in addition to some small- to medium-sized failures on other nearby slopes. Although these secondly landslides were not large enough to block or divert the Bhote Koshi River channel, they are an indication of the continued instability of the entire landslide area (Fig. 12 (6)). It is important to note that the current level of the Bhote Koshi River is more than 10 m lower than the uppermost fluvial/diamicton boundary on the east slope of the station due to continued river incision driven by tectonic uplift of the central Himalaya (Figs. 7b, e and 10a). Thus, with continued tectonically driven erosional incision, adjacent valley slopes become more susceptible to mass wasting and the landslide hazard persists.

Stability analysis of the large paleo-landslide site west of Tatopani Border Station

Because earthquakes occur frequently in Nepal, the international border stations along the Bhote Koshi River Valley remain

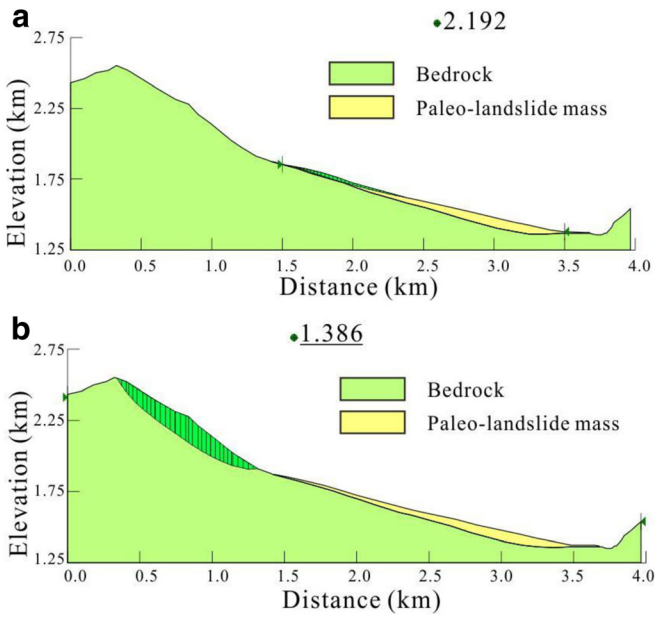

Fig. 13 Simulated static stability state of the paleo-landslide (*number* above legend refers to factor of safety (*FOS*); stippled green area indicates the part with smallest FOS). **a** Sliding surface restricted to the base of the paleo-landslide area. **b** Sliding surface chosen without any restriction

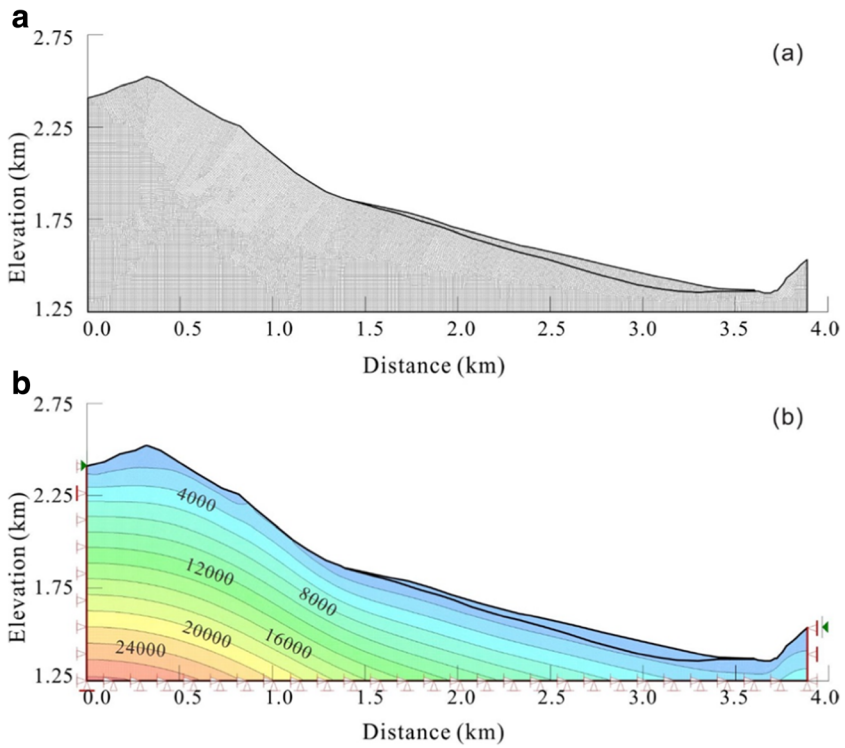

Fig. 14 **a** Finite element mesh of the model; **b** effective vertical stress contours obtained from initial static analysis (kPa)

vulnerable to future ground shaking and associated mass wasting. To better understand the potential impact of future earthquakes on the stability of the large paleo-landslide site west of Tatopani, a two-dimensional numerical model utilizing GeoStudio software was generated. The GeoStudio software is widely used for evaluating the stability of landslides (Gasmo et al. 2000; Rahardjo et al. 2001; Zhang et al. 2005; Chung et al. 2010; Wang et al. 2011; Borja et al. 2012). The analytical method was introduced in detail by Krahn (2004).

The relative indices of geotechnical properties for simulation are listed in Table 1. The values of which are based on conventional soil and rock mechanic experiments, including the ring method, the direct shear test, and compression and tensile tests. For the soil mechanic experiments, undisturbed soil samples were collected. For the friction angle and cohesion, their values are obtained by fitting straight line based on the data pairs (shear strength and normal stress) from the direct shear tests. The dip angle and vertical intercept of the straight line are the friction angle and cohesion, respectively.

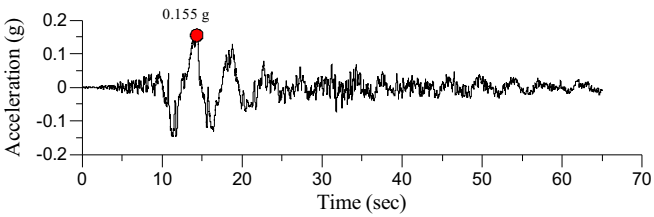

Fig. 15 Time history in the E-W direction of the 2015 M_w 7.8 Gorkha earthquake recorded in the Kathmandu Basin, Nepal

Static stability analysis of the paleo-landslide

The GeoStudio Slope/W module is commonly used to quantify the stability of the slope. In the numerical simulations, the limit equilibrium method presented by Morgenstern and Price (1965) was used to determine the factor of safety. In our analyses, ground water conditions were not considered because there is no existing groundwater database for the study area (despite obvious evidence for a shallow water table in the steep slopes surrounding the paleo-landslide mass where visible seeps and springs are common).

Figure 13 shows two typical results of a static analysis. When the sliding surface is restricted to the base of the paleo-landslide area, the minimum factor of safety (FOS) of the interface between the landslide accumulation and bedrock substrate is 2.192 (Fig. 13a). When the program automatically chooses a slip surface without restriction, the corresponding factor of safety is 1.386 (Fig. 13b). It thus can be concluded that the paleo-landslide is stable under the static state. However, according to the positions of the potential sliding surface presented by the simulation results, failure is prone to occur within the uppermost basal part of the landslide body (Fig. 13a) and near the steep scarps (Fig. 13b) with extra triggering factors such as an earthquake.

The Quake/W module of GeoStudio is based on a dynamic finite element analysis and was then used to calculate the dynamic stresses during earthquake loading. In this analysis, the numerical model is divided automatically by Quake/W into a finite element mesh (FEM) with 22,914 nodes and 22,777 elements (each element = 10 m). The initial static slope stresses were then simulated based on the initial static analysis. The finite element mesh of the model and effective vertical stresses are shown in Fig. 14.

Table 2 PGA used to scale the initial record in the analysis

No	PGA	Type	Source
1	0.22 *g*	PGA triggered by the M_w 7.3 aftershock in the station	USGS (2015)
2	0.35 *g*	PGA triggered by the M_w 7.8 mainshock in the epicentral area	USGS (2015)
3	0.48 *g*	PGA with 10% probability of exceedance in 50 years in the station	Zhang et al. (1999)
4	0.55 *g*	PGA with 10% probability of exceedance in 50 years in the station	Ram and Wang (2013)
5	0.70 *g*	Two times of PGA 2	Effect of topographical amplification

Equivalent linear dynamic analysis

The slope stresses change with time as horizontal ground motions are added. Quake/W can compute element dynamic stresses during the earthquake; the computed results are then saved on time steps and used as stress environments in the next step. The inputted ground motion, as a critical factor in the analysis, is discussed in detail below.

Despite the large magnitude of the 2015 M_w 7.8 Nepal (Gorkha) earthquake, the earthquake sequence was poorly recorded (Aydan and Ulusay 2015). Only one strong ground motion time-series has so far been provided by the USGS (www.strongmotioncenter.org). The data were recorded by the strong motion instrument (KATNP, Fig. 1) located in the middle of the Kathmandu Basin (27.730°N, 85.336°E), which is about 60 km from the epicenter. Because the profile used for simulation is nearly an E-W direction (Fig. 5), an E-W horizontal component record is used in this study (Fig. 15).

Of course, the accelerogram recorded in the Kathmandu basin is different from the seismic record of the earthquake that caused the large paleo-landslide. Therefore, it is necessary to scale the initial record with the maximum ground acceleration (PGA) that is likely to shake the station in the future (Anastasiadis et al. 2004).

The USGS preliminary estimation of PGA in the epicentral area was about 0.35 *g*. The Tatopani station is in a similar tectonic environment and thus may experience the same intensity of ground motion in the future. Also, the PGA (0.22 *g*) triggered by the largest Gorkha sequence aftershock of M_w 7.3 (http://earthquake.usgs.gov/archive/product/shakemap/us20002926/us/1435877532354/download/pga.jpg), which was near the border station site, was also used in this study.

A PGA estimate with 10% probability of exceedance in 50 years (i.e., recurrence period of 475 years), which is a basis for seismic design in Nepal, is used to consider the effect of topographic amplification (Celebi 1987). Because no related data could be collected by the authors, test results in other locations were considered for determining the scaling-up factor due to topographic amplification in the Tatopani study area. According to the available PGA data at different elevations in the Qingchuan area of the Longmenshan along the southeastern margin of the Qinghai Tibet Plateau (Wang et al. 2009), PGA values induced by a single microseismic event are one to three times larger along the up-slope than at the top of a slope in the same area. This site effect is more obvious (three times greater) when the slope orientation is the same as the propagation direction of the seismic waves. This is consistent with other research results showing that seismic acceleration increases with slope inclination (Griffiths and Bollinger 1979). In our analyses, a median of one to three times scaling-up was used. The PGAs used to scale the initial record are shown in Table 2.

It should be noted that the PGAs listed in Table 2 are only the estimated values that could be experienced by the station in the future and are simply used to illustrate the problem.

Permanent deformation analysis

SLOPE/W can use the finite element stresses obtained from the QUAKE/W dynamic analysis to examine the stability and permanent deformation of the slope to earthquake shaking using a procedure based on the Newmark method (Newmark 1965). According to this method, sliding of a failed mass occurs whenever the inertial force of the mass exceeds the frictional resistance along the sliding surface. The frictional resistance is characterized by yield acceleration. Newmark permanent deformation of slope is calculated by double integration of the difference between mass acceleration and yield acceleration (Krahn 2004). The maximum calculated permanent deformations are shown in Table 3, and the corresponding sliding surfaces are shown in Fig. 16.

The results suggest that factors of safety decrease with PGA increasing, while the maximum permanent deformation obviously increases (Table 3). Potential failures are always more likely to occur near the main scarp area during future earthquakes (Fig. 16), which will also influence the stability of the paleo-landslide body further downslope.

The FOS variation as a function of time is indicated in Fig. 17, which reveals that the minimum FOS almost always occurs during the time of 14.2 s to 14.3 s.

Table 3 Minimum factors of safety and maximum permanent deformation obtained from dynamic analysis

No.	PGA (*g*)	No. of slip face	Min. FOS	Time of min. FOS (s)	Max. permanent deformation (m)
1	0.22	2	0.938	14.2	0.141
2	0.35	2	0.770	14.2	3.338
3	0.48	3	0.654	14.2	9.177
4	0.55	1	0.602	14.3	13.148
5	0.70	1	0.515	14.3	23.144

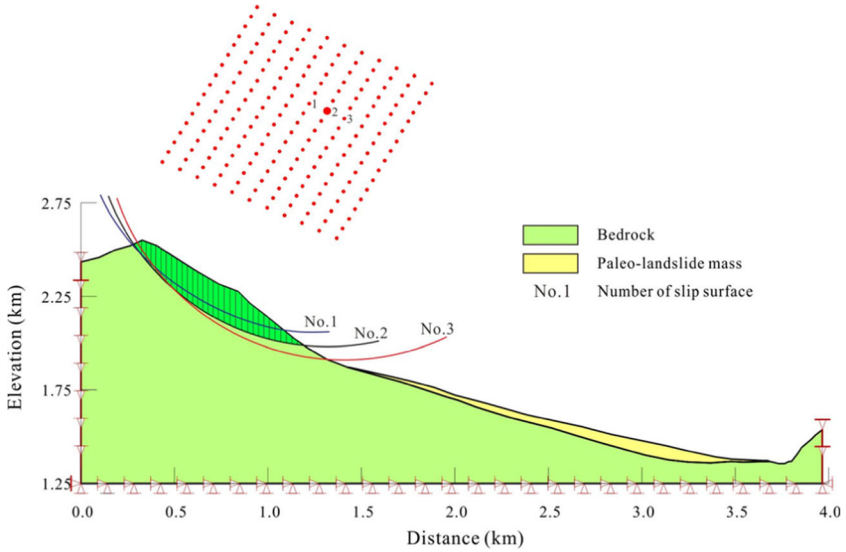

Fig. 16 Corresponding sliding surfaces of the maximum permanent deformation

When the PGA is set as 0.22 *g*, FOS is less than 1 for a short time (Fig. 17) and the Newmark deformation is small (Table 3), indicating a stable slope with only small- or medium-size failures. This is consistent with the field investigation results: only small- to

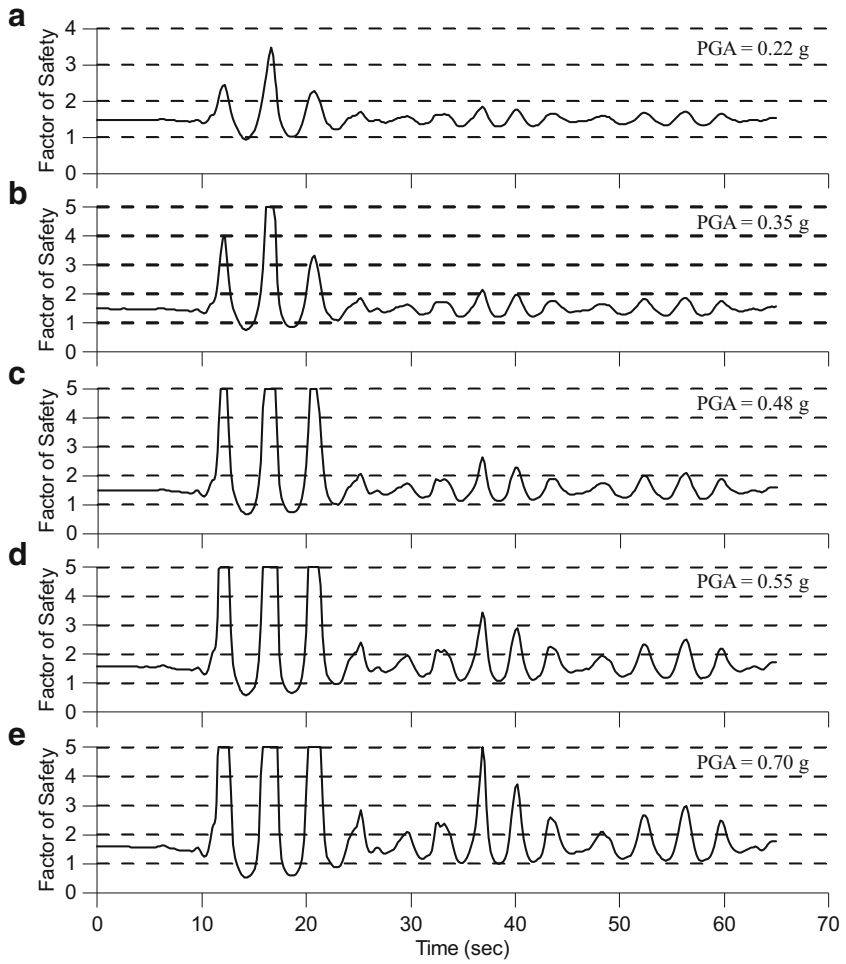

Fig. 17 Factor of safety vs. time with different PGA-scaled ground motion

medium-scale failures such as collapses on steep scarps and shallow secondary landslides on the south scarp were triggered by the 2015 Gorkha earthquake sequence.

However, the min FOS reduces rapidly with PGA increasing (Table 3 and Fig. 17). This indicates that the slope would be unstable when the PGA exceeds 0.35 *g*, which could be experienced in the future and potentially reactivating the entire paleo-landslide area. This should be taken into consideration for future earthquake-resistant design of the border station.

Discussion and conclusions

Mountainous terrain is modified and reduced by earthquake shaking-induced mass wasting and erosion. Slope stability and its relationship to earthquake-induced ground shaking is an important research area (Oka and Wu 1990; Duncan 2000; Whitman 2000; Griffiths et al. 2009; Yuan et al. 2013; Yuan et al. 2015). Landslides and debris flows induced by strong coseismic ground shaking are potentially the most destructive earthquake effects, as evidenced by the serious damage and casualties resulting from the 2005 Kashmir, 2008 Wenchuan, and 2015 Gorkha earthquakes (Keefer et al. 2006; Dai et al. 2011; Yuan et al. 2010; Collins and Jibson 2015).

Recent earthquakes with M7+ in the Himalaya are a testament to the ongoing convergence between India and southern Eurasia (Liu et al. 2015; Pandey and Molnar 1988; Biham 1995; Biham and Ambraseys 2005; Wesnouskey et al. 1999; Szeliga et al. 2010). Future earthquakes pose a threat to Nepalese infrastructure and societal development. This is also true for the critical trade corridor along the Bhote Koshi River valley and its international border stations.

The 2015 M_w 7.8 Gorkha (Nepal) earthquake and its aftershocks caused nearly 9000 deaths and more than 23,000 injuries and triggered thousands of landslides and collapses in the steep, rugged topography of Nepal. The results of our field investigation indicate that different types of geohazards occur around the construction site of the border station, a key project of Nepal. The site of the border station is located at the toe of a large paleo-landslide with a multistage history of hillslope modification and catastrophic collapse. Some new slope failures and many fissures were created by the 2015 Nepal earthquake sequence, indicating that it is possible for the large paleo-landslide area to be further reactivated by future earthquakes.

Simulated results suggest that the large paleo-landslide area is stable without seismic loading. However, it could be destroyed by large failures if the PGA exceeds 0.35 *g*, which might occur during future earthquakes. This important conclusion should be seriously considered by planners of all future construction projects at the Tatopani border station and more widely along the vital Bhote Koshi transport and trade corridor between Nepal and China. In addition, because of the border station's position directly below and east of a steep unvegetated cliff containing jointed and foliated bedrock (Fig. 7a) with 500 m+ of relief and with average slope gradients of 70%, the station will always be vulnerable to falling rocks (Fig. 7b–d) and other collapsed masses from cliff-face outcrops and loose talus that may have been repositioned during the Gorkha events and are now more unstable. In addition, the relentless fluvial erosion and undercutting of the northern side of the sedimentary bench that the Tatopani site is built upon will continue to threaten the station, especially during flood events. Thus, we suggest that relocating the border station should be seriously considered. Otherwise, strict disaster management plan should be designed and implemented. Because the upper Bhote Koshi River valley is flanked by steep slopes with abundant landslide scars on both the east and west sides, any future development along the transport corridor should be focused in areas of greatest slope stability. A favorable site for border station relocation appears to exist along the Araniko Highway only 2.5 km downstream (south) in an area immediately south of the village of Hindi on the east bank of the Bhote Koshi River, well above river level (Fig. 2). This area appears favorable because the river valley is wider with gentler slopes on the east side (gradients between 30 and 40%), and landslides did not occur upslope from this area during the 2015 Gorkha events. In addition, paleo-landslides appear to be absent on the surrounding terraced and wooded slopes above this site suggesting long-term stability.

Acknowledgements

This work was financially supported by the Basic Science Fund of the Institute of Geology, China Earthquake Administration (IGCEA1604 and IGCEA1609), for which grateful appreciation is expressed.

References

Ader T, Avouac JP, Liu-Zeng J, Lyon-Caen H, Bollinger L, Galetzka J, Genrich J, Thomas M, Chanard K, Sapkota SN, Rajaure S, Shrestha P, Ding L, Flouzat M (2012) Convergence rate across the Nepal Himalaya and interseismic coupling on the main Himalayan thrust: implications for seismic hazard. J Geophys Res 117(B4). doi:10.1029/2011JB009071

Anastasiadis A, Klimis N, Makra K, Margaris B (2004) On seismic behaviour of a 130 m high rockfill dam: an integrated approach. 13th Conference on Earthquake engineering, Vancouver, Canada, 2933p

Aydan Ö, Ulusay R (2015) A quick report on the 2015 Gorkha (Nepal) earthquake and its geo-engineering aspects

Bettinelli P, Avouac JP, Flouzat M, Jouanne F, Bollinger L, Willis P, Chitrakar GR (2006) Plate motion of India and interseismic strain in the Nepal Himalaya from GPS and DORIS measurements. J Geodesy 80:567–589

Bhandary NP, Yatabe R, Dahal RK, Hasegawa S, Inagaki H (2013) Areal distribution of large-scale landslides along highway corridors in Central Nepal. Georisk: Assessment and Management of Risk for Engineered Systems and Geohazards 7(1):1–20

Bhattarai D, Tsunaki R, Mishra AN (2002) Water and risk. In: Proceedings of Asia High Summit, 6–10 May 2002, ICIMOD. Nepal

Biham R (1995) Location and magnitude of the 1833 Nepal earthquake and its relation to the rupture zones of contiguous great Himalayan earthquakes. Curr Sci 69:101–128

Biham R, Ambraseys N (2005) Apparent Himalayan slip deficit from the summation of seismic moments for Himalayan earthquakes 1500-2000. Curr Sci 88:1658–1663

Bilham R, Larson K, Freymueller J, Project Idylhim members (1997) GPS measurements of present-day convergence across the Nepal Himalaya. Nature 386:61–64

Borja RI, White JA, Liu XY, Wu W (2012) Factor of safety in a partially saturated slope inferred from hydro-mechanical continuum modeling. Int J Numer Anal Meth Geomech 36:236–248. doi:10.1002/nag.1021

Celebi M (1987) Topographical and geological amplifications determined from strong-motion and aftershock records of the 3 March 1985 Chile earthquake. Bull Seism Soc Am 77:1147–1167

Chung MC, Tan CH, Chi SY, Ku CY, Su TW, Lee JF, Fei LY (2010) Monitoring and modeling of rainfall-induced landslides–a case study of Song-Mao landslide in central Taiwan. Conference on geology and slope hazards, p 372–381

Collins BD, Jibson RW (2015) Assessment of existing and potential landslide hazards resulting from the April 25, 2015 Gorkha, Nepal Earthquake Sequence: U.S. Geological Survey Open-File Report 2015–1142, 50 p., doi:10.3133/ofr20151142

Dai FC, Xu C, Yao X, Xu L, Tu XB, Gong QM (2011) Spatial distribution of landslides triggered by the 2008 MS 8.0 Wenchuan earthquake, China. J Asian Earth Sci 40(4):883–895

Duncan JM (2000) Factors of safety and reliability in geotechnical engineering. J Geotech Geoenviron 126(4):307–316. doi:10.1061/(ASCE)1090-0241(2000)126:4(307)

Gabet EJ, Burbank DW, Putkonen JK, Pratt-Sitaula BA, Ojha T (2004) Rainfall thresholds for landsliding in the Himalayas of Nepal. Geomorphology 63:131–143
Gansser A (1964) The geology of the Himalayas. Wiley Interscience, New York, 289 pp
Gasmo JM, Rahardjo H, Leong EC (2000) Infiltration effects on stability of a residual soil slope. Comput Geotech 26:145–165
Griffiths DW, Bollinger GA (1979) The effect of Appalachian Mountain topography on seismic waves. Bull Seismol Soc Am 69(4):1081–1105
Griffiths DV, Huang J, Fenton GA (2009) Influence of spatial variability on slope reliability using 2-D random fields. J Geotech Geoenviron 135(10):1367–1378. doi:10.1061/(ASCE)GT.1943-5606.0000099
Hasegawa S, Dahal RK, Yamanaka M, Bhandary NP, Yatabe R, Inagaki H (2009) Causes of large-scale landslides in the lesser Himalaya of Central Nepal. Environ Geol 57(6):1423–1434. doi:10.1007/s00254-008-1420-z
Hashash, YMA, Tiwari B, Moss RES, Asimaki D, Clahan KB, Kieffer DS, Dreger DS, Macdonald A, Madugo CM, Mason HB, Pehlivan M, Rayamajhi D, Acharya I, Adhikari B (2015) Geotechnical field reconnaissance: Gorkha (Nepal) earthquake of April 25, 2015 and related shaking sequence. Geotechnical Extreme Event Reconnaisance GEER Association Report No. GEER-040, Version 1.1, August 7, 2015, p 1–250
Kargel JS, Leonard GJ, Shugar DH, Haritashya UK, Bevington A, Fielding EJ, Fujita K, Geertsema M, Miles ES (2016) Geomorphic and geologic controls of geohazards induced by Nepal's 2015 Gorkha earthquake. Science 351:0036–8075. doi:10.1126/science.aac8353
Keefer DK, Wartman J, Ochoa CN, Rodriguez-Marek A, Wieczorek GF (2006) Landslides caused by the M 7.6 Tecomán, Mexico earthquake of January 21, 2003. Eng Geol 86(2):183–197
Krahn J (2004) Stability modeling with SLOPE/W: an engineering methodology, GEO-SLOPE/W International Ltd., Calgary, Alta., Canada
Le Fort P (1975) Himalayas: the collided range. Present knowledge of the continental arc. Am J Sci 275(1):44
Liu J, Ji C, Zhang JY, Zhang PZ, Zeng LS, Li ZF, Wang W (2015) Tectonic setting and general features of coseismic rupture of the 25 April 2015 Mw 7.8 Gorkha, Nepal earthquake. Chin Sci Bull 60:2640–2655 (in Chinese)
Morgenstern NR, Price VE (1965) The analysis of the stability of general slip surfaces. Geotechnique 15:79–93
Mugnier JL, Huyghe P (2006) The Ganges Basin geometry records a pre-15 Ma lithospheric isostatic rebound of the Himalaya. Geology 34:445–448
Newmark NM (1965) Effects of earthquakes on dams and embankments. Geotechnique 15:139–159
Oka Y, Wu TH (1990) System reliability of slope stability. J Geotech Eng 116(8):1185–1189. doi:10.1061/(ASCE)0733-9410(1990)116:8(1185)
Pandey MR, Molnar P (1988) The distribution of intensity of the Bihar-Nepal earthquake of 15 January 1934 and bounds on the extent of the rupture zone. J Nepal Geol Soc 5:23–45
Rahardjo H, Li XW, Toll DG, Leong EC (2001) The effect of antecedent rainfall on slope stability. Geotech Geol Eng 19:371–399
Ram TD, Wang G (2013) Probabilistic seismic hazard analysis in Nepal. Earthquake Eng Eng Vib 12:577–586. doi:10.1007/s11803-013-0191-z
Shanker D, Sharma ML (1998) Estimation of seismic hazard parameters for the Himalayas and its vicinity from complete data files. Pure Appl Geophys 152:267–279
Shroder JF, Bishop MP (1998) Mass movement in the Himalaya: new insights and research directions. Geomorphology 26:13–35
Szeliga W, Hough S, Martin S, Bilham R (2010) Intensity, magnitude, location, and attenuation in India for felt earthquake since 1762. Bull Seismol Soc Ame 100:570–584
Wang Y, Cao Z, Au SK (2011) Practical reliability analysis of slope stability by advanced Monte Carlo simulations in a spreadsheet. Can Geotech J 48:162–172. doi:10.1139/T10-044
Wang Y, Xu H, Luo Y, Wu J (2009) Study of formation conditions and toss motion program of high landslides induced by earthquake. Chin J Rock Mech Eng 28(11):2360–2368 (in Chinese)
Wesnouskey SG, Kumar S, Mohindra R, Thakur VC (1999) Uplift and convergence along the Himalayan frontal thrust of India. Tectonics 18:967–976
Whitman RV (2000) Organizing and evaluating uncertainty in geotechnical engineering. J Geotech Geoenviron 126(7):583–593. doi:10.1061/(ASCE)1090-0241(2000)126:7(583)
Yuan RM, Deng QH, Cunningham D, Xu C, Xu XW, Chang CP (2013) Density distribution of landslides triggered by the 2008 Wenchuan earthquake and their relationships to peak ground acceleration. Bull Seismol Soc Am 103(4):2344–2355
Yuan RM, Tang CL, Deng QH (2015) Effect of the acceleration component normal to the sliding surface on earthquake-induced landslide triggering. Landslides 12(2):335–344. doi:10.1007/s10346-014-0486-9
Yuan RM, Xu XW, Chen GH, Tan XB, Klinger Y, Xing HL (2010) Ejection landslide at northern terminus of Beichuan rupture triggered by the 2008 mw 7.9 Wenchuan earthquake. Bull Seismol Soc Am 100(5B):2689–2699
Zhang P, Yang ZX, Gupta HK, Bhatia SC, Shedlock KM (1999) Global seismic hazard assessment program (GSHAP) in continental Asia. Ann Geofis 42(6):1167–1190
Zhang LL, Zhang LM, Tang WH (2005) Rainfall-induced slope failure considering variability of soil properties. Geotechnique 55(2):183–188

G. Wu · R. Yuan (✉) · Q. Zhou (✉) · X. Yang
Key Laboratory of Active Tectonics and Volcano,
Institute of Geology, China Earthquake Administration,
Beijing, 100029, People's Republic of China
e-mail: yuanrenmao@ies.ac.cn
e-mail: zqcsb@163.com

D. Cunningham
Department of Environmental Earth Science,
Eastern Connecticut State University,
83 Windham Street, Willimantic, CT 06226, USA

X. Zeng
Earthquake Administration of Jiangxi Province,
Nanchang, 330039, China